

KINETIC ANALYSIS OF BIOMOLECULAR INTERACTIONS USING LABEL-FREE BIOSENSORS

Yung-Shin Sun¹ and X. D. Zhu²

¹*Department of Physics, Fu-Jen Catholic University, New Taipei City, Taiwan*

²*Department of Physics, University of California at Davis, Davis, California, USA*

□ *One key advantage of label-free biosensors involves the monitoring of binding between biomolecules. However, a number of experimental artifacts may lead to complicated real-time curves that do not fit well to a simple Langmuir model. As a result, the quality of the kinetic data must be improved to obtain accurate reaction rates. By carefully designing experiments, collecting the data, and processing the data, issues arising from signal drift, nonspecific binding, mass-transport effect in solution, mass-transport effect on surface, and curve fitting may be avoided or resolved. Using a label-free oblique-incidence reflectivity difference biosensor, key processes required to obtain reliable kinetic data and accurate reaction rates are described.*

Keywords biosensor, kinetics, label-free, Langmuir model, reaction rates

INTRODUCTION

Label-free biosensors provide an important platform for characterizing biomolecular interactions. Various techniques including surface plasmon resonance (SPR), interference, and ellipsometry have been applied in designing and constructing such devices.^[1–7] These biosensors measure the changes in refractive index and/or thickness due to captured biomolecules near the sensing surface. They are capable of *in-situ* and real-time monitoring interactions between binding partners. Most importantly, by following the kinetic curves, the reaction rates and thermodynamic constants can be derived.^[8–10] These values are crucial in understanding the underlying mechanisms of certain reactions. For example, in screening for potential drugs against diseases, knowing the association and dissociation rates helps pharmaceutical companies to better test the efficiency, stability, and durability of these candidates.

In a typical SPR- or ellipsometry-based biosensor, one biomolecule is immobilized on a solid substrate (e.g., glass) as the target, and the other

Address correspondence to Yung-Shin Sun, Department of Physics, Fu-Jen Catholic University, No.510, Zhongzheng Rd., Xinzhuang Dist., New Taipei City 24205, Taiwan (R.O.C.). E-mail: 089957@mail.fju.edu.tw

Color versions of one or more of the figures in the article can be found online at www.tandfonline.com/list.

one, the probe, is in a solution. The association phase begins as the probe is injected into the fluidic chamber and flows across the target-covered surface. In the dissociation phase, the probe solution is replaced with running buffer. With more and more biosensors commercially available (most of them are SPR-based),^[11,12] such processes are automatically controlled to monitor the association and dissociation between probe and target molecules. While these instruments are easy to operate, the derived kinetic data sometime does not fit well to a simple Langmuir model. For example, fitting with the simple one-to-one model may lead to inaccurate rate constants that are significantly different from those derived from solution-based methods such as isothermal titration calorimetry (ITC).^[13–17] There are a number of experimental processes that can possibly complicate the kinetic analysis, including signal drift from instrument and/or ambient, non-specific binding, mass transport from probes and/or targets, and fitting model. These artifacts can be avoided by carefully designing the experiment, collecting the data, and processing the data. After such improvements, the kinetic data can be fitted well with the simple or sophisticated Langmuir models to obtain the reactions rate close to those from solution-based methods.^[10,12,18–20]

There were only few references reporting how to improve real-time biosensor analysis with a focus on SPR-based instruments. Myszka et al. provided technical notes on how to improve the quality of optical biosensor data in order to characterize the mechanism and rate constants associated with molecular interactions.^[21] They suggested that many of the artifacts associated with binding data can be minimized or eliminated by designing the experiment properly, collecting data under optimum conditions, and processing the data with reference surfaces. The same group also reviewed the current state of biosensor technology and highlighted recent advances in data acquisition and analysis.^[12] Special attention was paid to improving biosensor data, mass transport effects, detecting small-molecule binding, and membrane surfaces.

In this article, using another label-free biosensor, ellipsometry-based oblique-incidence reflectivity difference (OI-RD) microscopy, key processes required to obtain kinetic data and accurate reaction rates are addressed. Particular attention was paid to signal drift, nonspecific binding, mass-transport effect in solution, mass-transport effect on surface, and curve fitting. Different from SPR-based biosensors,^[12,21] this OI-RD microscopy incorporates a microarray platform to provide more flexible experimental design and more information. For example, by printing target molecules with different concentrations, the mass-transport effect on surface may be systematically studied.

OI-RD MICROSCOPY

The working principles of OI-RD microscopy were detailed in references.^[22–26] Basically, this method measures the changes in reflectivity difference between *p*- and *s*-polarized components of a laser beam in response to surface-captured biomolecules. Combining with microarrays, this biosensor provides a platform for label-free, *in-situ*, real-time, and high-throughput detections of various biomolecular interactions.^[27–37]

SIGNAL DRIFT

In monitoring real-time curves, signal drift can occur as a result of subtle changes in the ambient conditions and/or the instrument. Optical components, such as mirrors and lenses, are sensitive to ambient temperature. Therefore, in a long-term run (>4 hr), temperature variation may cause drift. Moreover, when injecting probe solutions, changes in ambient refractive index also lead to drift. To avoid such artifacts, referencing against neighboring blank substrates is required. In a typical OI-RD experiment, signals from targets and their neighboring references are monitored, and the binding curves are derived by subtracting the average reference signal from the target signal. Considering the binding of

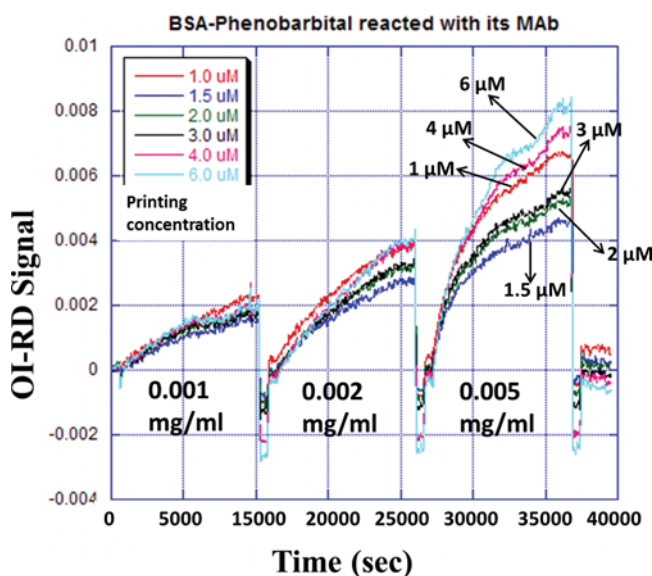


FIGURE 1 Binding curves of surface-immobilized bovine serum albumin-conjugated phenobarbital reacting with its solution-phased antibody after subtraction of the average reference signal. Printing concentrations from 1 μ M to 6 μ M, and probe concentrations of 0.001 mg/mL, 0.002 mg/mL, and 0.005 mg/mL were used sequentially.

surface-immobilized bovine serum albumin-conjugated phenobarbital to its solution-phased antibody as an example,^[38] the raw binding curves containing signal drift and variation were very rough (data not shown). This phenomenon would affect data fitting. Figure 1 shows the binding curves after subtracting out the average reference signal from two blank substrates. Printing concentrations from 1 μM to 6 μM and probe concentrations of 0.001 mg/mL, 0.002 mg/mL, and 0.005 mg/mL were used sequentially.^[38] The sensing surface was regenerated between two bindings to strip off captured probes. These curves seem smoother and are therefore more suitable for subsequent analysis.

NONSPECIFIC BINDING

Microarrays provide a platform for high-throughput and parallel detection of biomolecular interactions. After target molecules are immobilized on functionalized solid substrates (e.g., epoxy- or amine-coated glass slides), surface blocking is required to reduce nonspecific binding between probes and unprinted areas. The nonspecific binding contributes to reference signals, which in turn lead to artifact probe-target bindings after referencing. These curves do not fit well to the simple one-to-one or other sophisticated models. In microarray applications, bovine serum albumin is commonly and widely used to block amine- or epoxy-coated slides because it is inexpensive and easy to use.^[39,40] Using a fluorescent scanner and an OI-RD microscope, the blocking efficiency of bovine serum albumin on epoxy-functionalized substrates was characterized, and it was found that a bovine serum albumin concentration of 0.05% (0.5 mg/mL or 10 μM) could give a blocking efficiency of 98% and the bovine serum albumin-blocking step took only 5 min to be complete (data to be published elsewhere). Blocking reagents such as succinic anhydride (SA), highly fluorinated organosilane, and others commercially available are also applicable to reduce nonspecific binding in microarrays.^[40–42]

MASS-TRANSPORT EFFECT IN SOLUTION

Due to the nature of surface-based biosensors, probe molecules diffuse and propagate through the bulk solution to reach and bind to surface-immobilized targets. This mass-transport effect was reported to affect the kinetic analysis.^[43–45] Using an iterative computer model, Glaser et al. numerically studied the kinetics of association and dissociation between soluble probes and immobilized targets on or near the SPR sensing surface.^[43] The transition between mass transport-controlled processes and reaction-controlled processes was described, and it was concluded that,

to measure high rate constants, the bound probes should be eluted with second probes of low molecular weight. Schuck et al. presented a new method, based on a phenomenological two-compartment approximate description of transport, to analyze biosensor data.^[44] The results indicated the extent to which the experimental binding progress was mass-transport controlled and whether or not the rate constants might be validly extracted from the data. Kusnezow et al. reported using a mathematical model, derived within the framework of two-compartment model, to quantitatively analyze the experimental data from typical antibody microspot assays.^[45] They found that the assay-based reactions were slowed down by several orders of magnitude as compared with the corresponding well-stirred bulk reactions.

This mass-transport effect can, to some extent, be overcome by continuously flowing fresh solution across the sensing surface. Flow rates are important for supplying enough fresh probes to surface targets but not causing too high shear stress. This parameter depends on both the volume of fluidic chamber and the concentration of probes. Higher flow rates are required in a bigger reaction chamber and a lower probe concentration. Experiments were performed to study the binding between surface-immobilized polyvinyl alcohol-conjugated 2,4-dinitrophenol and its solution-phased antibody at different concentrations (data not shown).^[46] Different flow rates of 0 mL/min, 0.01 mL/min, 0.03 mL/min, 0.1 mL/min, and 0.3 mL/min were used, which, in a 0.4 mL fluidic chamber, means that the probe solutions were refreshed in infinite time, 40 min, 13 min, 4 min, and 1.3 min, respectively. At probe concentrations of 113 nM and 28 nM, the flow rate did not affect the binding kinetics. The real-time curve of a 0.3 mL/min flow rate was similar to that without flowing. However, as the probe concentration was lowered to 7 nM, the reaction rate depended significantly on the flow rate. This mass-transport limitation could yield a two-fold difference in the association rates between a 0.3 mL/min flow rate and no flow. Therefore, to eliminate the mass-transport effect in solution, an adequate flow rate (at least one refreshing of probes in 10 min) is required. On the other hand, the shear stress near the sensing surface is proportional to the flow rate, so a too high rate may strip off bound probes due to an elevated stress.

MASS-TRANSPORT ON THE SURFACE

On the sensing surface, the mass-transport effect of probes through the target layers also affects the kinetic analysis.^[47,48] Probes diffuse across surface-deposited targets to find their binding epitopes or ligands. The extent to which this mass-transport limitation affects reaction rates depends on the density of surface targets. Peterson et al. studied how target density affected the hybridization to unlabeled probe oligonucleotides containing

mismatched sequences. Using a SPR biosensor, their results of kinetic, equilibrium, and temperature-dependent studies were significantly different from those obtained in solution-based reactions. Using a total internal reflection fluorescence microscope, Michel et al. investigated the kinetics of DNA hybridization on glass substrates. They concluded that the surface density of immobilized DNA was crucial in designing microarrays. It should be low enough so that hybridization was not hindered by tightly packed surface targets, but sufficiently high to provide enough surface molecules for probe-bindings. Figure 2 shows the association curves of 100 nM streptavidin reacting with surface-immobilized biotin-bovine serum albumin conjugates at different printing concentrations.^[35] The reaction rates (in $k_{on}[c]$, where k_{on} is the association rate and $[c]$ is the probe concentration) and the changes in OI-RD signal were plotted against the printing concentration, as shown in Figure 3. A dashed line indicated the printing concentration where a “side-one” monolayer of bovine serum albumin molecules was formed on the surface. Clearly, the OI-RD signal increased with printing concentration because more target molecules became available to probes. The reaction rate, in contrast, decreased with increasing printing concentration, and a sudden drop occurred near the dashed line (printing concentration = 3 μ M). This suggested that the association rate decreased

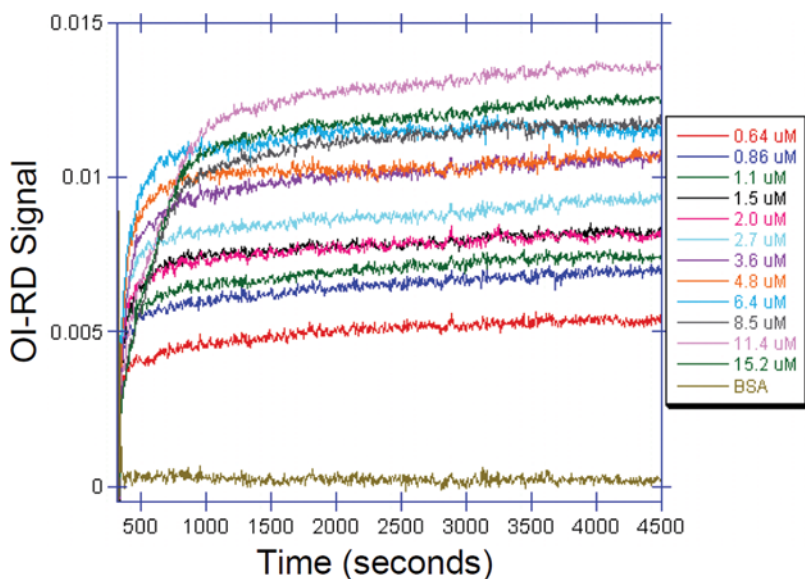


FIGURE 2 Association curves of streptavidin at 100 nM reacting with surface-immobilized biotin-bovine serum albumin conjugates at different printing concentrations. To acquire the reaction rate, each curve was fitted to the simple one-to-one Langmuir model.^[35]

© Taylor & Francis, Ltd. Reproduced by permission of Taylor & Francis, Ltd. Permission to reuse must be obtained from the rightsholder.

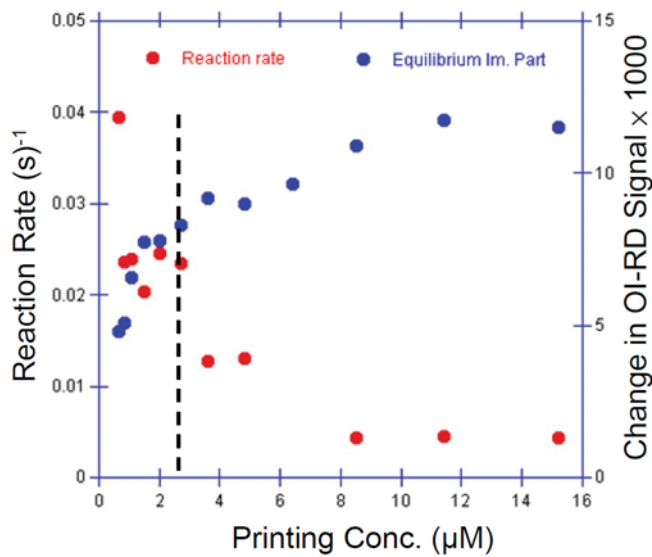


FIGURE 3 Reaction rate ($k_{om}[c]$) and change in OI-RD signal versus printing concentration due to streptavidin binding to biotin-bovine serum albumin targets at different printing concentrations.^[35]

© Taylor & Francis, Ltd. Reproduced by permission of Taylor & Francis, Ltd. Permission to reuse must be obtained from the rightsholder.

because antibody probes had to diffuse and penetrate the bovine serum albumin molecules to bind to biotin targets. The reaction rate would be most accurate at printing concentrations less than but close to a critical value where a monolayer of targets was formed (i.e., 3 µM in this study). There is an optimal range of surface target density that should be experimentally derived and controlled: too high values may cause mass-transport effects, while too low values may decrease the detection limit.

CURVE FITTING

Even with attention paid to the above mentioned issues, the kinetic data may not fit well to the simple one-to-one Langmuir model. Possible reasons include steric hindrance caused by immobilization heterogeneity, and the bivalency of antibody probes when reacting with surface antigens. Under these circumstances, more sophisticated fitting models, such as one-to-two and two-to-one Langmuir models, are required to obtain accurate reaction rates.^[9,49–51] For example, Morton et al. reported using three methods for deriving kinetic constants from biosensor data: linearization, curve fitting using the integrated rate equation, and curve fitting using the numerical integration.^[49] Two complex systems, one including a two-state conformational change and a second involving surface heterogeneity, were generated for analysis. The results concluded that the lineariza-

tion method was inadequate for these systems, the integrated rate equation simulated surface heterogeneity very well, and the numerical integration was the only method providing accurate rate constants for both systems. Edwards et al. showed that the association data, especially at high probe concentrations, was better fitted with a double-exponential function.^[51] Possible models to this two-rate process included the presence of two distinct surface populations, a conformational change, and surface heterogeneity. In this study, to fit OI-RD signals, the Langmuir one-to-one and one-to-two models are used:^[34,46]

One-to-one, association

$$\theta(t) = \theta_{eq} [1 - \exp(-(k_{on}[A]_0 + k_{off})t)], \quad t \leq t_0; \quad (1)$$

One-to-one, dissociation

$$\theta(t) = \theta_{eq} [1 - \exp(-(k_{on}[A]_0 + k_{off})t_0)] \exp(-(t - t_0)k_{off}), \quad t \geq t_0; \quad (2)$$

One-to-two, association

$$\theta(t) = \theta_{eq} [\gamma^{(1)} (1 - \exp(-(k_{on}^{(1)}[A]_0 + k_{off}^{(1)})t)) + \gamma^{(2)} (1 - \exp(-(k_{on}^{(2)}[A]_0 + k_{off}^{(2)})t))], \quad t \leq t_0; \quad (3)$$

One-to-two, dissociation

$$\theta(t) = \theta_{eq} \left\{ \gamma^{(1)} [1 - \exp(-(k_{on}^{(1)}[A]_0 + k_{off}^{(1)})t_0)] \exp(-(t - t_0)k_{off}^{(1)}) + \gamma^{(2)} [1 - \exp(-(k_{on}^{(2)}[A]_0 + k_{off}^{(2)})t_0)] \exp(-(t - t_0)k_{off}^{(2)}) \right\}, \quad t \geq t_0. \quad (4)$$

In these equations, θ is the coverage, θ_{eq} is the equilibrium coverage, k_{on} is the association rate, k_{off} is the dissociation rate, $[A]_0$ is the probe concentration, γ is the occupation ratio, and the probe solution is replaced with buffer at $t = t_0$. Figures 4 and 5 show the real-time binding curves of surface-immobilized bovine serum albumin-conjugated 2,4-dinitrophenol reacting with its solution-phased antibody at different concentrations. The Langmuir one-to-one and one-to-two fittings were used in Figure 4 and 5, respectively. Clearly, as shown in Figure 4, the one-to-one model did not fit well to the kinetic data, especially for higher probe concentrations (226 nM and 452 nM). The fittings was much better in Figure 5, where the one-to-two model was used. Table 1 lists the fitting parameters. The one-to-one model provided an equilibrium dissociation constant (K_D) of 0.287 nM, which might not be accurate due to a poor fit. In the one-to-

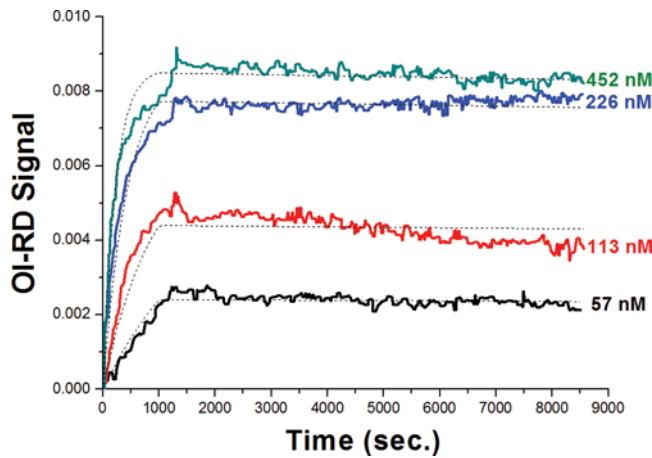


FIGURE 4 Real-time binding curves of surface-immobilized dinitrophenol-bovine serum albumin reacting with its solution-phased antibody. Dotted lines indicate Langmuir one-to-one fitting.

two model, site-one had a slightly higher occupation ratio of 0.58. The K_D values of bindings at site-one and site-two were 6.48 nM and less than 0.057 nM, respectively. For bindings at site-two, the dynamic off-rate was very small (less than $1.4 \times 10^{-6} \text{ s}^{-1}$), which indicated that reactions at this site had a stronger binding affinity than those at site-one. One possible explanation was that site-two targets ($\sim 42\%$ of all targets) provided direct bindings for probes, but site-one targets ($\sim 58\%$ of all targets) reacting with

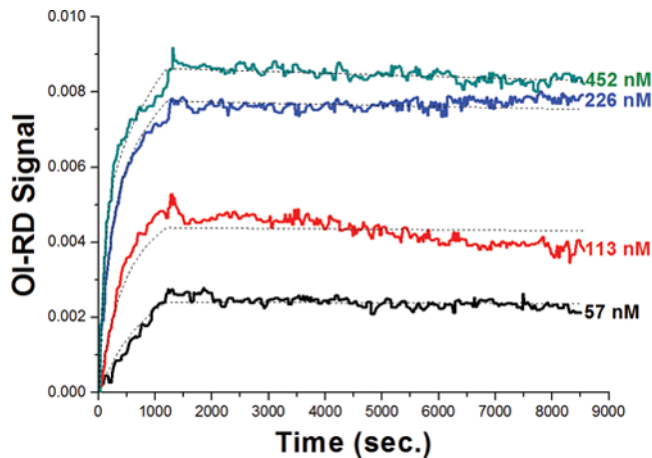


FIGURE 5 Real-time binding curves of surface-immobilized dinitrophenol-bovine serum albumin reacting with its solution-phased antibody. Dotted lines indicate Langmuir one-to-two fitting.

TABLE 1 One-to-one and one-to-two Langmuir fitting parameters to Dinitrophenol-bovine serum albumin reacting with its antibody

One-to-one	k_{on} (nMs) ⁻¹ 9.98×10^{-6}	k_{off} (s) ⁻¹ 2.86×10^{-6}	K_D (nM) 0.287			
One-to-two $\gamma^{(1)} = 0.58$	$k_{on}^{(1)}$ (nMs) ⁻¹ 1.76×10^{-6}	$k_{off}^{(1)}$ (s) ⁻¹ 1.14×10^{-5}	$K_D^{(1)}$ (nM) 6.48	$k_{on}^{(2)}$ (nMs) ⁻¹ 2.46×10^{-5}	$k_{off}^{(2)}$ (s) ⁻¹ $< 1.40 \times 10^{-6}$	$K_D^{(2)}$ (nM) < 0.057

 k_{on} : association rate k_{off} : dissociation rate K_D : equilibrium dissociation constant γ : occupation ratio¹site-one²site-two

probes was somehow affected by mass-transport effects within target molecules.

CONCLUSIONS

Label-free biosensors are important tools in characterizing biomolecular interactions as well as understanding the binding mechanisms. As more and more biosensors become commercially available, they may be used without careful attention to experimental design and how reaction rates are derived. Under such circumstances, due to a number of experimental artifacts, the kinetic data is sometimes questionable. To avoid such drawbacks, experimental design, data collection, and data processing should be particularly addressed. This article reports solutions to signal drift, non-specific binding, mass-transport effect in solution, mass-transport effect on surface, and curve fitting on data analysis. These issues were addressed experimentally to provide better understanding. For example, signal drift can be corrected with substrate referencing, nonspecific binding can be avoided with blocking, mass-transport effect was minimized with suitable flow rate and controlled target concentration, and different curve-fitting models were applied to obtain accurate reaction rates. With careful design and procedures, high-quality biosensor data may be obtained to provide accurate kinetic and thermodynamic constants.

FUNDING

The authors are thankful for financial support from NIH-R01-HG003827 (X. D. Zhu) and Taiwan MOST 101-2112-M-030-003-MY3 (Y. S. Sun).

REFERENCES

1. Sun, Y.S. Optical Biosensors for Label-Free Detection of Biomolecular Interactions. *Instrum. Sci. Technol.* **2014**, *42*, 109–127.
2. Bottazzi, B.; Fornasari, L.; Frangolho, A.; Giudicatti, S.; Mantovani, A.; Marabelli, F.; Marchesini, G.; Pellacani, P.; Therisod, R.; Valsesia, A. Multiplexed Label-Free Optical Biosensor for Medical Diagnostics. *J. Biomed. Opt.* **2014**, *19*, 17006.
3. Deng, J.; Song, Y.; Wang, Y.; Di, J. Label-Free Optical Biosensor based on Localized Surface Plasmon Resonance of Twin-Linked Gold Nanoparticles Electrodeposited on ITO Glass. *Biosens. Bioelectron.* **2010**, *26*, 615–619.
4. Huang, H.; He, C.; Zeng, Y.; Xia, X.; Yu, X.; Yi, P.; Chen, Z. A Novel Label-Free Multi-throughput Optical Biosensor based on Localized Surface Plasmon Resonance. *Biosens. Bioelectron.* **2009**, *24*, 2255–2259.
5. Schmitt, K.; Schirmer, B.; Hoffmann, C.; Brandenburg, A.; Meyrueis, P. Interferometric Biosensor based on Planar Optical Waveguide Sensor Chips for Label-Free Detection of Surface Bound Bioreactions. *Biosens. Bioelectron.* **2007**, *22*, 2591–2597.
6. Acharya, G.; Chang, C.L.; Savran, C. An Optical Biosensor for Rapid and Label-Free Detection of Cells. *J. Amer. Chem. Soc.* **2006**, *128*, 3862–3863.
7. Endo, T.; Kerman, K.; Nagatani, N.; Takamura, Y.; Tamiya, E. Label-Free Detection of Peptide Nucleic Acid-DNA Hybridization using Localized Surface Plasmon Resonance based Optical Biosensor. *Anal. Chem.* **2005**, *77*, 6976–6984.
8. Myszka, D.G. Kinetic analysis of macromolecular interactions using surface plasmon resonance biosensors. *Curr. Opin. Biotechnol.* **1997**, *8*, 50–57.
9. Rich, R.L.; Cannon, M.J.; Jenkins, J.; Pandian, P.; Sundaram, S.; Magyar, R.; Brockman, J.; Lambert, J.; Myszka, D.G. Extracting Kinetic Rate Constants from Surface Plasmon Resonance Array Systems. *Anal. Biochem.* **2008**, *373*, 112–120.
10. Day, Y.S.; Baird, C.L.; Rich, R.L.; Myszka, D.G. Direct Comparison of Binding Equilibrium, Thermodynamic, and Rate Constants Determined by Surface- and Solution-Based Biophysical Methods. *Protein Sci.* **2002**, *11*, 1017–1025.
11. Cooper, M.A. Optical Biosensors: Where Next and How Soon?. *Drug Discov. Today* **2006**, *11*, 1061–1067.
12. Rich, R.L.; Myszka, D.G. Advances in Surface Plasmon Resonance Biosensor Analysis. *Curr. Opin. Biotechnol.* **2000**, *11*, 54–61.
13. Krainer, G.; Broecker, J.; Vargas, C.; Fanghanel, J.; Keller, S. Quantifying High-Affinity Binding of Hydrophobic Ligands by Isothermal Titration Calorimetry. *Anal. Chem.* **2012**, *84*, 10715–10722.
14. O'Shannessy, D.J.; Brigham-Burke, M.; Sonesson, K.K.; Hensley, P.; Brooks, I. Determination of Rate and Equilibrium Binding Constants for Macromolecular Interactions using Surface Plasmon Resonance: Use of Nonlinear Least Squares Analysis Methods. *Anal. Biochem.* **1993**, *212*, 457–468.
15. Parker, K.M.; Stalcup, A.M. Affinity Capillary Electrophoresis and Isothermal Titration Calorimetry for the Determination of Fatty Acid Binding with Beta-cyclodextrin. *J. Chromatogr. A* **2008**, *1204*, 171–182.
16. Talhout, R.; Villa, A.; Mark, A.E.; Engberts, A.B. Understanding Binding Affinity: a Combined Isothermal Titration Calorimetry/Molecular Dynamics Study of the Binding of a Series of Hydrophobically Modified Benzamidinium Chloride Inhibitors to Trypsin. *J. Am. Chem. Soc.* **2003**, *125*, 10570–10579.
17. Zeder-Lutz, G.; Altschuh, D.; Geysen, H.M.; Trifilieff, E.; Sommermeyer, G.; Van Regenmortel, M. H. Monoclonal Antipeptide Antibodies: Affinity and Kinetic Rate Constants Measured for the Peptide and the Cognate Protein Using a Biosensor Technology. *Mol. Immunol.* **1993**, *30*, 145–155.
18. Yoo, S.; Myszka, D.G.; Yeh, C.; McMurray, M.; Hill, C.P.; Sundquist, W.I. Molecular Recognition in the HIV-1 Capsid/Cyclophilin A Complex. *J. Mol. Biol.* **1997**, *269*, 780–795.
19. Joss, L.; Morton, T.A.; Doyle, M.L.; Myszka, D.G. Interpreting Kinetic Rate Constants from Optical Biosensor Data Recorded on a Decaying Surface. *Anal. Biochem.* **1998**, *261*, 203–210.
20. Leder, L.; Llera, A.; Lavoie, P.M.; Lebedeva, M.I.; Li, H.; Sekaly, R.P.; Bohach, G.A.; Gahr, P.J.; Schlievert, P.M.; Karjalainen, K.; Mariuzza, R.A. A Mutational Analysis of the Binding of Staphylococcal Enterotoxins B and C3 to the T Cell Receptor Beta Chain and Major Histocompatibility Complex Class II. *J. Exp. Med.* **1998**, *187*, 823–833.

21. Myszka, D.G. Improving Biosensor Analysis. *J. Mol. Recognit.* **1999**, *12*, 279–284.
22. Fei, Y.Y.; Landry, J.P.; Sun, Y.S.; Zhu, X.D.; Luo, J.T.; Wang, X.B.; Lam, K.S. A Novel High-Throughput Scanning Microscope for Label-Free Detection of Protein and Small-Molecule Chemical Microarrays. *Rev. Sci. Instrum.* **2008**, *79*, 013708.
23. Landry, J.P.; Gray, J.; O'Toole, M.K.; Zhu, X.D. Incidence-Angle Dependence of Optical Reflectivity Difference from an Ultrathin Film on Solid Surface. *Opt. Lett.* **2006**, *31*, 531–533.
24. Landry, J.P.; Zhu, X.D.; Gregg, J.P. Label-Free Detection of Microarrays of Biomolecules by Oblique-Incidence Reflectivity Difference Microscopy. *Opt. Lett.* **2004**, *29*, 581–583.
25. Zhu, X.D. Comparison of Two Optical Techniques for Label-Free Detection of Biomolecular Microarrays on Solids. *Opt. Commun.* **2006**, *259*, 751–753.
26. Zhu, X.D.; Landry, J.P.; Sun, Y.S.; Gregg, J.P.; Lam, K.S.; Guo, X.W. Oblique-Incidence Reflectivity Difference Microscope for Label-Free High-Throughput Detection of Biochemical Reactions in a Microarray Format. *Appl. Opt.* **2007**, *46*, 1890–1895.
27. Fei, Y.; Landry, J.P.; Li, Y.; Yu, H.; Lau, K.; Huang, S.; Chokhawala, H.A.; Chen, X.; Zhu, X.D. An Optics-Based Variable-Temperature Assay System for Characterizing Thermodynamics of Biomolecular Reactions on Solid Support. *Rev. Sci. Instrum.* **2013**, *84*, 114102.
28. Fei, Y.Y.; Landry, J.P.; Sun, Y.S.; Zhu, X.D.; Wang, X.B.; Luo, J.T.; Wu, C.Y.; Lam, K.S. Screening Small-Molecule Compound Microarrays for Protein Ligands without Fluorescence Labeling with a High-Throughput Scanning Microscope. *J. Biomed. Opt.* **2010**, *15*, 016018.
29. Fei, Y.Y.; Schmidt, A.; Bylund, G.; Johansson, D.X.; Henriksson, S.; Lebrilla, C.; Solnick, J.V.; Boren, T.; Zhu, X.D. Use of Real-Time, Label-Free Analysis in Revealing Low-Affinity Binding to Blood Group Antigens by *Helicobacter Pylori*. *Anal. Chem.* **2011**, *83*, 6336–6341.
30. Fei, Y.Y.; Sun, Y.S.; Li, Y.H.; Lau, K.; Yu, H.; Chokhawala, H.A.; Huang, S.S.; Landry, J.P.; Chen, X.; Zhu, X.D. Fluorescent Labeling Agents Change Binding Profiles of Glycan-Binding Proteins. *Mol. Biosyst.* **2011**, *7*, 3343–3352.
31. Landry, J.P.; Fei, Y.; Zhu, X.; Ke, Y.; Yu, G.; Lee, P. Discovering Small Molecule Ligands of Vascular Endothelial Growth Factor that Block VEGF-KDR Binding using Label-Free Microarray-Based Assays. *Assay Drug Dev. Technol.* **2013**, *11*, 326–332.
32. Landry, J.P.; Fei, Y.Y.; Zhu, X.D. Simultaneous Measurement of 10,000 Protein-Ligand Affinity Constants Using Microarray-Based Kinetic Constant Assays. *Assay Drug Dev. Technol.* **2012**, *10*, 250–259.
33. Landry, J.P.; Sun, Y.S.; Guo, X.W.; Zhu, X.D. Protein Reactions with Surface-Bound Molecular Targets Detected by Oblique-Incidence Reflectivity Difference Microscopes. *Appl. Opt.* **2008**, *47*, 3275–3288.
34. Sun, Y.S.; Landry, J.P.; Fei, Y.Y.; Zhu, X.D. Effect of Fluorescently Labeling Protein Probes on Kinetics of Protein-Ligand Reactions. *Langmuir* **2008**, *24*, 13399–13405.
35. Sun, Y.S.; Landry, J.P.; Fei, Y.Y.; Zhu, X.D. An Oblique-Incidence Reflectivity Difference Study of the Dependence of Probe-Target Reaction Constants on Surface Target Density Using Streptavidin-Biotin Reactions as a Model. *Instrum. Sci. Technol.* **2013**, *41*, 535–544.
36. Sun, Y.S.; Luo, J.T.; Lam, K.S.; Zhu, X.D. Detection of Formation and Disintegration of Micelles by Oblique-Incidence Reflectivity Difference Microscopy. *Instrum. Sci. Technol.* **2013**, *41*, 545–555.
37. Sun, Y.S.; Zhu, X.D. Ellipsometry-Based Biosensor for Label-Free Detection of Biomolecular Interactions in Micro array Format. *Sensor Mater.* **2013**, *25*, 673–688.
38. Sun, Y.S.; Lam, K.S.; Zhu, X.D. Determination of Bovine Serum Albumin Conjugated Drugs by Immobilization as Microarrays and Oblique-Incidence Reflectivity Difference Microscopy. *Instrum. Sci. Technol.* **2014**, *42*, 475–485.
39. MacBeath, G.; Schreiber, S.L. Printing Proteins as Microarrays for High-Throughput Function Determination. *Science* **2000**, *289*, 1760–1763.
40. Taylor, S.; Smith, S.; Windle, B.; Guiseppi-Elie, A. Impact of Surface Chemistry and Blocking Strategies on DNA Microarrays. *Nucleic Acids Res.* **2003**, *31*, e87.
41. Hsieh, H.Y.; Wang, P.C.; Wu, C.L.; Huang, C.W.; Chieng, C.C.; Tseng, F.G. Effective Enhancement of Fluorescence Detection Efficiency in Protein Microarray Assays: Application of a Highly Fluorinated Organosilane as the Blocking Agent on the Background Surface by a Facile Vapor-Phase Deposition Process. *Analyt. Chem.* **2009**, *81*, 7908–7916.
42. Shultz, M.A.; Ohdera, A.; MacManiman, J.; McGrath, C.M. Optimized Blocking Of Porous Nitrocellulose Films For Sensitive Protein Microarrays. *Biotechniques* **2013**, *54*, 223–225.

43. Glaser, R.W. Antigen-Antibody Binding and Mass Transport by Convection and Diffusion to a Surface: A Two-Dimensional Computer Model of Binding and Dissociation Kinetics. *Anal. Biochem.* **1993**, *213*, 152–161.
44. Schuck, P.; Minton, A.P. Analysis of Mass Transport-Limited Binding Kinetics in Evanescent Wave Biosensors. *Anal. Biochem.* **1996**, *240*, 262–272.
45. Kusnezow, W.; Syagailo, Y.V.; Ruffer, S.; Klenin, K.; Sebald, W.; Hoheisel, J.D.; Gauer, C.; Goychuk, I. Kinetics of Antigen Binding to Antibody Microspots: Strong Limitation by Mass Transport to the Surface. *Proteomics* **2006**, *6*, 794–803.
46. Sun, Y.S.; Landry, J.P.; Fei, Y.Y.; Zhu, X.D.; Luo, J.T.; Wang, X.B.; Lam, K.S. Macromolecular Scaffolds for Immobilizing Small Molecule Microarrays in Label-Free Detection of Protein-Ligand Interactions on Solid Support. *Anal. Chem.* **2009**, *81*, 5373–5380.
47. Sigmundsson, K.; Masson, G.; Rice, R.; Beauchemin, N.; Obrink, B. Determination of Active Concentrations and Association and Dissociation Rate Constants of Interacting Biomolecules: an Analytical Solution to the Theory for Kinetic and Mass Transport Limitations in Biosensor Technology and its Experimental Verification. *Biochemistry* **2002**, *41*, 8263–8276.
48. Jennissen, H.P.; Zumbink, T. Mass Transport-Free Protein Adsorption Kinetics in Biosensor Systems. *Faseb J.* **2001**, *15*, A531–A531.
49. Morton, T.A.; Myszka, D.G.; Chaiken, I.M. Interpreting Complex Binding Kinetics from Optical Biosensors: A Comparison of Analysis by Linearization, the Integrated Rate Equation, and Numerical Integration. *Anal. Biochem.* **1995**, *227*, 176–185.
50. Morton, T.A.; Myszka, D.G. Kinetic Analysis of Macromolecular Interactions using Surface Plasmon Resonance Biosensors. *Meth. Enzymol.* **1998**, *295*, 268–294.
51. Edwards, P.R.; Gill, A.; Pollard-Knight, D.V.; Hoare, M.; Buckle, P.E.; Lowe, P.A.; Leatherbarrow, R.J. Kinetics of Protein-Protein Interactions at the Surface of an Optical Biosensor. *Anal. Biochem.* **1995**, *231*, 210–217.